Atomic Layer Deposition of Ultrathin Copper Metal Films from a Liquid Copper(I) Amidinate Precursor

Zhengwen Li, Antti Rahtu,[a] and Roy G. Gordon*,[z]

Department of Chemistry and Chemical Biology, Harvard University, Cambridge 102138, Massachusetts, USA

We report a method for producing thin, completely continuous and highly conductive copper films conformally inside very narrow holes with aspect ratios over 35:1 by atomic layer deposition (ALD). Pure copper thin films were grown from a novel copper(I) amidinate precursor, copper(I) *N,N′*-di-sec-butylacetamidinate, and molecular hydrogen gas as the reducing agent. This copper precursor is a liquid during vaporization because its melting point (77°C) is lower than its vaporization temperature (90–120°C). Thus, the transport of the precursor vapor is very reproducible and controllable. Carbon and oxygen impurities were below 1 atom %. The growth per cycle varied from 1.5–2 Å/cycle on SiO_2 or Si_3N_4 surfaces but was only 0.1–0.5 Å/cycle on metallic Ru, Cu, and Co surfaces. On oxide surfaces, copper atoms form isolated copper crystallites that merge into rough polycrystalline films after more deposition cycles. On Ru and Co metal surfaces ALD Cu nucleates densely, forming smooth and strongly adherent films that are continuous even for films as thin as 4 atomic layers. With 4 nm Cu deposited on 2 nm Ru substrates, the sheet resistance is below 50 Ω/□, which is low enough for making seed layers for electroplating Cu interconnect wires.
© 2006 The Electrochemical Society. [DOI: 10.1149/1.2338632] All rights reserved.

Copper is replacing aluminum in microelectronic interconnections because copper circuits are faster and last longer. The copper is electroplated inside trenches and holes in insulators.[1] A thin continuous copper seed layer is needed before electroplating Cu. In current technology, sputtering is used to deposit these seed layers. However, it is difficult to sputter completely conformal and uniform copper seed layers into the increasingly narrow trenches and vias in modern interconnects. Chemical methods are likely to solve this problem for making the tiny microelectronic and nanoelectronic devices expected in the future.[2] Atomic layer deposition (ALD) is well known for depositing conformal and continuous films into structures with very high aspect ratios. ALD deposition is one of the most promising techniques to enable nanoscale device fabrication due to its precise thickness control of conformal and uniform coatings over large areas.[3] ALD processes have been developed for many metal oxides, nitrides, and sulfides,[4] while use of ALD for metals such as copper have been hindered mainly by the scarcity of appropriately reactive and stable metal precursors.

Being volatile, thermally stable, and highly reactive are three basic requirements for good ALD precursors for copper deposition. The copper precursor needs to be volatile enough to be carried as a vapor from the vapor source to the deposition chamber. It must be stable without significant decomposition at the source temperature for many months. In order to yield highly pure films, the precursor must not decompose during the time that it is adsorbed on the hot surface of a substrate for a few seconds, while awaiting the next pulse of reducing gas. Furthermore, the precursor should react with the substrate surface and with the surface prepared by the complementary reagent (such as H_2 to produce metal films). The surface reactions should be self-limiting, thus yielding layer-by-layer growth of films with high conformality and precise thickness control.

Copper films could be deposited by ALD using hydrogen atoms as the reducing agent.[5] However, hydrogen atoms recombine quickly on surfaces, so they cannot be transported deep into trenches or holes with high aspect ratios. An ALD process using stable molecular reducing agents, such as hydrogen molecules, is needed to coat uniformly inside narrow holes. Also, there are concerns about plasma damage which can degrade the quality of the films or substrates.

A low-temperature deposition process (<200°C) is desirable, in order to achieve smooth and continuous thin copper films. Previously used precursors have not demonstrated reactivity to molecular-reducing agents at low temperatures.

Comparison and Characterization of Copper Precursors

Cu thin films made from ALD techniques have been reported using several different copper sources. Their physical properties have been summarized in Table I and their structures are shown in Fig. 1. They include copper monochloride $[(CuCl)_3$, Fig. 1a],[6] Cu β-diketonate derivatives, such as copper (II) bis(2,4-pentanedionate) $[Cu(acac)_2$, Fig. 1b],[7] copper bis(2,2,6,6-tetramethyl-3,5-heptanedionate) $[Cu(thd)_2$, Fig. 1c],[8] and copper(II) hexafluoroacetylacetonate hydrate $[Cu(hfac)_2 \cdot xH_2O$, Fig. 1d].[9] All these precursors have drawbacks. In the case of copper monochloride, zinc was used as the reducing agent, which caused contamination that is not acceptable for microelectronics applications. Also, the volatility of CuCl is so low that very high temperatures (>400°C) must be used to evaporate and transport the precursor. Cu β-diketonate derivatives have relatively low reactivity, which required high deposition temperatures (>300°C). Decomposition of the β-diketonate precursors incorporated carbon and oxygen impurities, which degraded the quality of the films. The fluorine content of $Cu(hfac)_2 \cdot xH_2O$ caused fluorine contamination of the films, reduced adhesion, and etching of substrates by by-product hydrofluoric acid (HF). All the Cu beta-diketonates have low reactivity with hydrogen due to their strong Cu–O bonds, which require high deposition temperatures, leading to rough Cu films with carbon and oxygen contamination. Our group reported a new copper(I) amidinate as ALD Cu precursor, *N,N′*-di-*iso*-propylacetamidinato copper(I) $\{[Cu(^iPr\text{-}amd)]_2$, Fig. 1e}.[8] The advantage of this precursor is that it has enough reactivity with molecular hydrogen to deposit pure copper metal films at relatively low temperature (~200°C). The disadvantage of this precursor is its high melting point (147°C), so that it sublimes from its solid phase in the reservoir. The vapor pressure and thus the evaporation rate depend on the powder size, which is not reproducible. Copper sources with lower melting points are desirable, because they are easier to purify, carry fewer solid particles into the deposition zone, and have constant, high vapor pressures. In this paper we report the growth of copper films from a copper precursor with a low melting point so that it evaporates from the liquid state and yields high-quality films.

We can vary the six alkyl groups outside of the copper(I) amidinate dimer molecules to tune the physical properties and find the best candidate for ALD of copper. Details about the synthesis and

[a] Present address: Vaisala OYJ, Vantaa, Finland.
[z] E-mail: Gordon@chemistry.harvard.edu
* Electrochemical Society Active Member.

Table I. Physical properties of different copper compounds.

Precursor name	Melting point (°C)	Temperature of $T_{1/2}$ from TG	Evaporation rate of Cu atoms at 100°C [nmol/(cm² min)]	Equilibrium vapor pressure (Torr/°C)	Enthalpy of sublimation (kJ/mole)
CuCl, a	430	~700	0.87	—	—
Cu(acac)$_2$, b	285(dec)	252	0.91	—	98.5
Cu(thd)$_2$, c	198(dec)	—	2.33	~0.02/50	105.7
Cu(hfac)$_2$·xH$_2$O, d	130–134	145	2280	~0.4/20	58.0
[Cu(^{i}Pr-amd)]$_2$, e	147	241	15.8	0.03/70	82.4
[Cu(^{n}Pr-amd)]$_2$, f	65	264	7.12	0.03/80	79.5
[Cu(^{s}Bu-amd)]$_2$, g	77	234	38.8	0.23/95	58.4

characterization of a dozen copper(I) amidinates have been reported elsewhere.[10] Here two of these candidates are listed in Fig. 1 for comparison with other copper precursors.

Thermal gravimetric analysis (TGA) is helpful in characterizing the volatilities and thermal stabilities of precursors.[11] The temperature at which half of the precursor was evaporated in normal temperature-ramped (10 K/min) TGA curve ($T_{1/2}$) is one way to compare volatilities.[12] These $T_{1/2}$ values are given in Table I. The very volatile fluorinated precursor, Cu(hfac)$_2$, has the lowest $T_{1/2}$ value, while the low-volatility CuCl has the highest. The others are intermediate in volatility, within a temperature range that is generally useful for ALD. The nonvolatile residue of the copper amidinate precursors is less than 1%, indicating that they have adequate thermal stability for vaporization.

Isothermal TGA was also used to study more quantitatively the evaporation kinetics of these copper compounds. In these experiments, the temperature of the TGA furnace was kept constant for 15 min, while the rate of mass loss by evaporation is measured. Then the temperature is increased by 10 K and is held steady again for 15 min. From the slope of the TG curve, the average evaporation rate was calculated at each temperature. Figure 2 shows the isothermal TGA data at 100°C for different copper compounds. It is clear that copper monochloride, a, has the lowest vaporization rate, only 0.87 nmol/(cm²-min), so it is difficult to use for ALD depositions. Cu(acac)$_2$, b, vaporizes only slightly faster, 0.91 nmol/(cm²-min). Cu(thd)$_2$, c, has a reasonable vaporization rate, 2.33 nmol/(cm²-min), but it is not thermally stable and decomposes at around 190°C. Because of the fluorination of its methyl groups, Cu(hfac)$_2$, d, has a much higher vaporization rate than Cu(acac)$_2$. [Cu(^{i}Pr-amd)]$_2$, e, has a reasonable vaporization rate, 15.8 nmol/(cm²-min), but it is still a solid at a bubbler temperature of 100°C. By changing the alkyl groups of the amidinate ligand, we found the two low-melting copper amidinates which are listed in Fig. 1. [Cu(^{n}Pr-amd)]$_2$, f, and [Cu(^{s}Bu-amd)]$_2$, g, have melting points of 65 and 77°C, respectively. They can be evaporated from their liquid phases during vapor deposition. [Cu(^{n}Pr-amd)]$_2$ has an evaporation rate of 7.1 nmol/cm²-min, while Cu(^{s}Bu-amd)$_2$ has the fastest vaporization

rate, 38.8 nmol/(cm²-min), among these amidinates. Moreover, Cu(^{s}Bu-amd)]$_2$ is very stable, having a half-life around 33 days at 190°C in benzene-d$_6$ solution.[10]

The evaporation enthalpies of different precursors were calculated from isothermal thermogravimetric (TG) data taken at different temperatures. Figure 3 shows the logarithm of the rate of weight loss as a function of $1000/T$. The enthalpy of evaporation was calculated from the slope. Cu amidinates d, e, and f have enthalpies of 82.4, 79.5, and 58.4 kJ/mol, respectively. This trend indicates decreased packing density and reduced intermolecular interactions going from d to f. The enthalpy of 58.0 kJ/mol for sublimation of Cu(hfac)$_2$·xH$_2$O is the lowest among all the copper precursors, while CuCl is almost nonvolatile. As a check of this measurement method, isothermal TG was measured for phenanthrene and its sublimation enthalpy was 83.2 kJ/mol, which agreed quite well with the literature values.[13]

Equilibrium vapor pressure was measured during the sublimation process for purifying the compounds, as another measure of the complexes' volatilities. Cu(hfac)$_2$·xH$_2$O is the most volatile compound, having a vapor pressure of ~0.4 Torr at 20°C. The vapor pressures of Cu(^{i}Pr-amd)$_2$, Cu(^{s}Bu-amd)$_2$, and Cu(^{n}Pr-amd)$_2$ were lower (see Table I), but these copper(I) amidinates are sufficiently volatile for use in vapor deposition. Among them, Cu(^{s}Bu-amd)$_2$ is the most promising candidate for chemical vapor deposition (CVD) and ALD applications, having sufficient volatility, thermal stability, and reactivity with molecular hydrogen.

ALD Experiments

Cu(^{a}Bu-amd)$_2$ was selected as the copper source for the ALD experiments due to its suitable physical properties discussed above. The hallmark of ALD self-limiting reaction is that the amount of material deposited (growth per cycle) first increases with the precursor exposure but then levels out to approach a constant value. The exposure is defined as the product of the precursor partial pressure
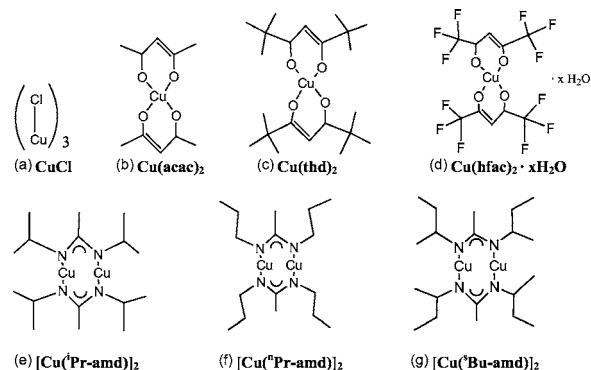

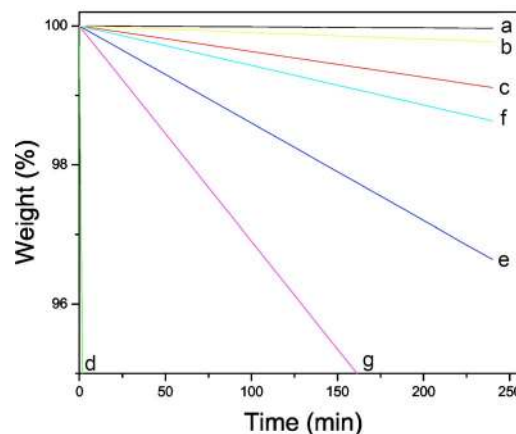**Figure 1.** Structures of Cu precursors for CVD and ALD Cu applications.

Figure 2. (Color online) Isothermal TG analysis at 100°C of different CVD and ALD copper precursors. The labels correspond to those in Fig. 1.
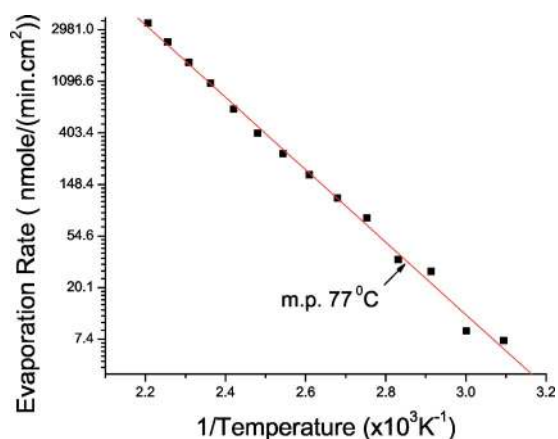
Figure 3. Evaporation kinetics of $[Cu(^sBu\text{-}amd)]_2$ by TG analysis. Isothermal for 15 min at each temperature, and then stepwise increase 10°C to higher temperature isothermal TG. The evaporation enthalpy from the slope is 58.4 kJ/mol.

and the time that it is exposed to the surface.[14] The exposure is proportional to the number of collisions of the precursor with the surface. Changes in the exposure can be made in three different ways: increasing the precursor dose by increasing the precursor bubbler temperature, by using multiple doses at fixed precursor temperature, and by increasing the precursor exposure time in the deposition chamber. Partial pressure and time were both varied, and the growth per cycle on ALD deposited Al_2O_3 substrates was plotted as a function of their product (Fig. 4a), based on 1000 cycles. The growth per cycle increases with increasing exposure to the copper precursor. The growth per cycle saturates at larger exposures, achieving a constant, saturated value of about 0.9 Å per cycle. The lower points were taken in the flow-through mode, in which the precursor flowed over the substrate and was pumped away immediately with exposure time of ~30 ms, while the higher exposure points were taken when the copper precursor was trapped inside the reactor with exposure times varying from 1 to 4 s. The growth per cycle was greatly enhanced by just lengthening the precursor exposure time with the same amount of precursor introduced to the reactor. The slow approach to saturation may be due to heterogeneous surface sites, some of which react quickly, while other surface sites need more collisions before the precursor can adsorb and react to form a saturated surface.

The effect of hydrogen to the growth per cycle was shown in Fig. 4b in flow-through conditions, in which both Cu precursor and H_2 flowed through the reactor and were pumped away continuously. The exposure of H_2 was hundreds of times larger than that of the copper precursor, leading to completely saturated growth at every point even with the smallest hydrogen exposure tested.

One advantage of ALD over CVD is that the deposits can be uniform over large areas. Figure 4c shows the plot of the growth per cycle on Ru as a function of distance from the precursor inlet. The deposition rate is uniform over a 12 cm distance.

The growth behavior can be affected by many factors, such as the surface chemistry, whether it is –OH terminated or –H terminated, the precursor exposure, deposition temperatures, etc. ALD Cu deposition showed different growth mechanisms on oxides and nitrides, compared to growth on metallic surfaces. Figure 5 shows the film thickness as a function of growth cycle numbers on ALD Al_2O_3 surfaces (Fig. 5a) and on metal Ru substrates (Fig. 5b), respectively. On ALD-deposited Al_2O_3, ALD-deposited HfO_2, and thermal silicon oxide surfaces, the growth per cycle is initially ~2 Å/cycle, a relatively high value. As the oxide surface was gradually covered by copper, the growth slowed down and approached 0.4–0.5 Å/cycle when the surface was totally covered by copper. In contrast, the growth per cycle is linear on Ru substrates, with 0.11 Å/cycle for
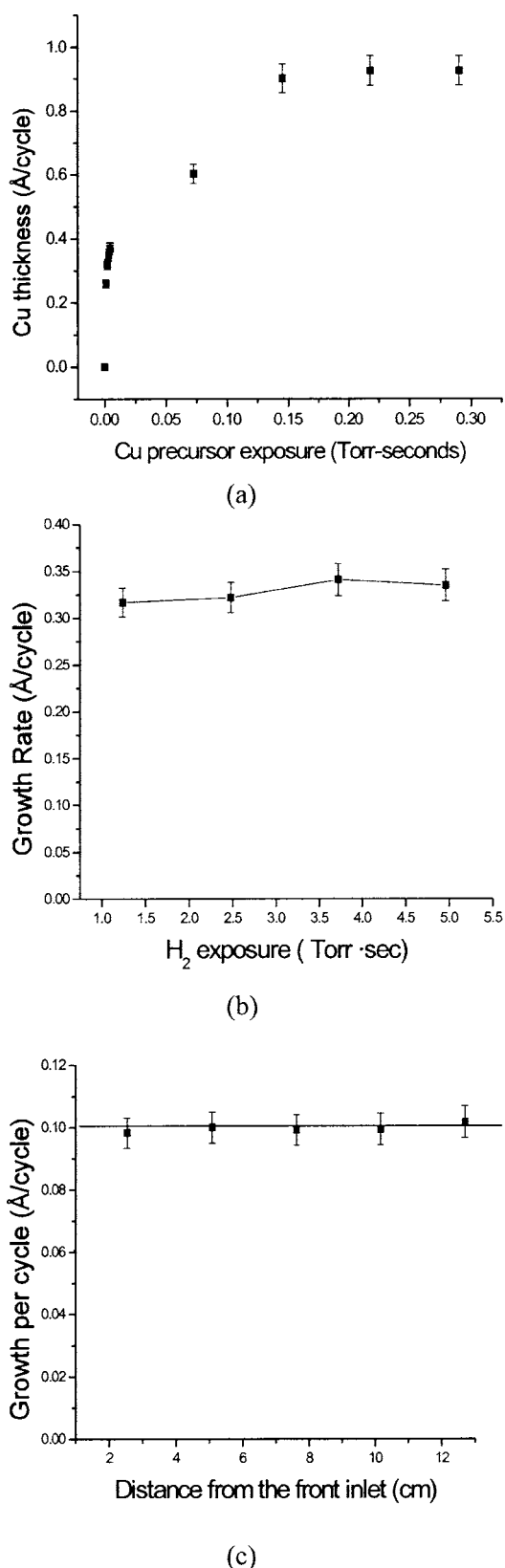

(a)

(b)

(c)

Figure 4. Growth per cycle of ALD Cu (a) as a function of Cu precursor exposure on ALD-deposited Al_2O_3, (b) as a function of H_2 exposure on ALD-deposited Al_2O_3, and (c) as a function of substrate location on Ru substrates.

less than fully saturated copper exposures. Table II lists the growth per cycle of ALD copper on different substrates. On metallic Ru,
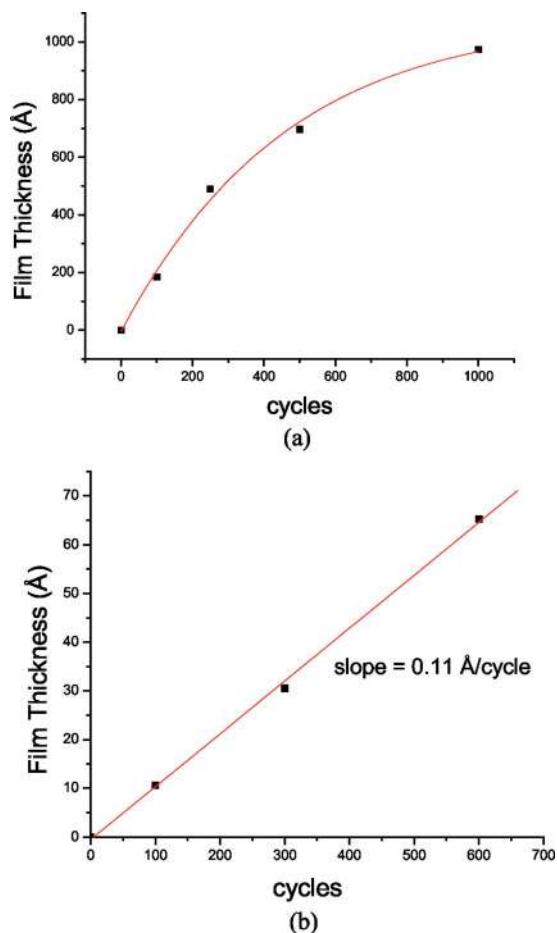
Figure 5. (Color online) The growth behavior of ALD Cu (a) on Al_2O_3 and (b) on Ru substrates.

Co, and Cu the growth per cycle is between 0.1 and 0.5 Å/cycle, much lower than on oxide or nitride surfaces. Transition-metal surfaces may catalyze some ALD processes. However, there is no catalytic effect in this case. Keeping other deposition conditions the same, the control experiments showed no Cu deposition on Ru or Co surface when only Cu precursor was introduced to the reactor, without the reducing agent H_2. All the thickness data were from the Rutherford backscattering spectrum (RBS), assuming bulk density for Cu films.

Properties of the ALD Copper Films

The nanostructure of very thin films (film thickness <10 nm) was studied by transmission electron microscopy (TEM) on thin SiO_2 TEM grids. Figure 6a shows ALD Cu films with an average

Table II. The growth per cycle of ALD Cu on different substrates.

Substrate	Growth per cycle (Å/cycle)	$[Cu(^sBu\text{-}amd)]_2$ Exposure (Torr·sec)
Al_2O_3/SiO_2	1.90 (based on 100 cycles)	0.15
Si_3N_4	1.50 (based on 60 cycles)	0.19
WN	0.54 (based on 30 cycles)	0.28
Ru	0.11 (based on 100 cycles)	0.16
Co	0.40 (based on 30 cycles)	0.28
Cu	~0.5 (from Al_2O_3 curve)	0.15
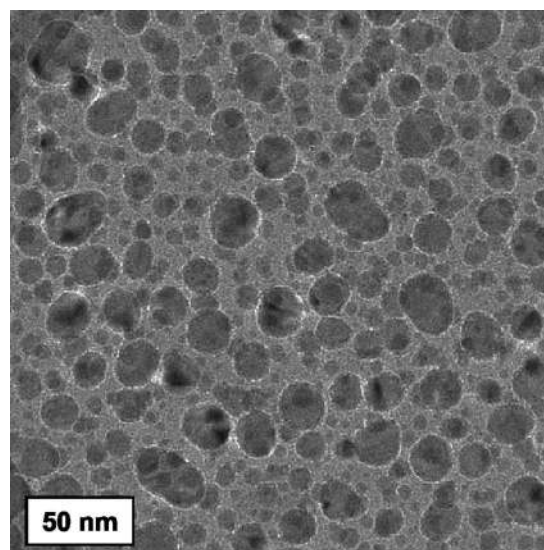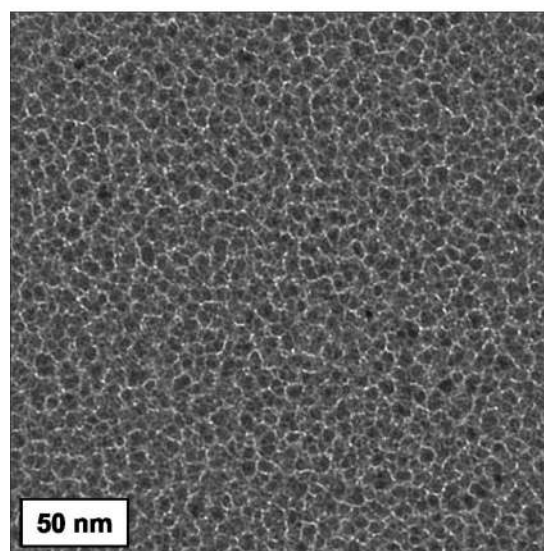
Figure 6. TEM study of Cu nucleation on different surfaces: (a) on SiO_2, 4.5 nm Cu, and (b) on Co, 2 nm Cu.

thickness of 4.5 nm, as measured by RBS. Cu grains are clearly seen as dark spots sitting on the transparent oxide membrane. As a comparison, 2 nm thick ALD Cu film already nucleated densely on the surface of a very thin PVD Co film (Fig. 6b).

One advantage of ALD over physical vapor deposition is the ability to grow films conformally and uniformly over high-aspect-ratio holes and trenches. Figure 7 shows a scanning electron microscopy (SEM) image of cleaved cross sections of Cu films inside UV ozone-treated oval holes in silicon. Although copper agglomerated to yield large grains (~ 100 nm) on the oxidized silicon surface, the copper is highly conformal inside the holes with aspect ratios $>35:1$. The thickness of the film on the bottom of the holes is equal to that on the top, demonstrating the ideal conformality of the ALD films.

Pure copper films could be made from the copper amidinate precursor with H_2 as the reducing agent. RBS was used to examine the impurities of the films. Figure 8 showed a RBS spectra of copper films deposited at 190°C, with a simulation curve (red line) having 1 atom % carbon impurity. Both carbon and oxygen impurities were

below the detection limit. For films grown above 300°C, a large amount (~ 10 atom %) of carbon was found in the films, which was due to thermal decomposition of the copper amidinate precursor at these high substrate temperatures.

The as-deposited copper films were polycrystalline according to X-ray diffraction (XRD) studies. As shown in Scheme 1, the as-deposited Cu films at 160°C were oriented at (111) direction, together with some (200) direction. As the deposition temperature increased to higher temperatures, the film crystallinity became more orientated in the (111) direction, which is typical for copper thin films.[15,16] This may be important for Cu interconnect applications because (111)-textured Cu films may have higher electromigration resistance.[17] The polycrystalline nature of the copper films was fur-
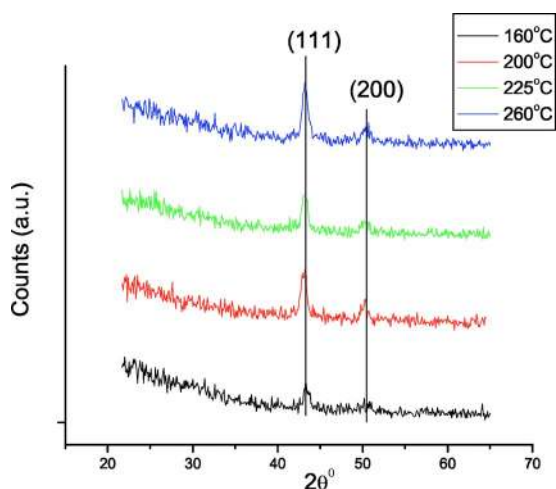
Scheme 1. (Color online) XRD of Cu film made by 1000 cycles of ALD on glass substrates (JCPDS card no.04-0836).

ther confirmed by high-resolution TEM. Figure 9 showed a copper grain deposited on SiO_2 TEM grids in Fig. 6. The copper lattices in different orientations are clearly shown in the grain, showing its polycrystalline structure.

Scotch tape tests showed that copper films grown on glass or on WN could be peeled off easily while the copper films adhered strongly on cobalt and ruthenium surfaces. Quantitative four-point bending experiments showed that the surface adhesion energies for all the interfaces of $Cu/Co/WN/SiO_2$ were greater than 31 J/m^2, which is much larger than 6 J/m^2 between TaN/SiO_2.[15,18]

The surface roughness of ALD Cu film was substrate-dependent. SEM was employed to study the surface morphology of the deposits. Figure 10 showed the film surfaces grown on different substrates in the same condition. The film deposited on glass (Fig. 10a) has the largest grains, which were separated from each other, while Fig. 10b showed copper film growth on ALD WN thin film. The grain size was smaller and the grain density increased, indicating slightly improved nucleation or inhibition of copper diffusion. Figure 10c showed the copper film deposited on the ALD cobalt surface. The grain size was the smallest and showed the densest nucleation. These SEM images agreed well with the TEM study in Fig. 6. On oxide surfaces, copper atoms adhere weakly and thus can diffuse rapidly and collect to form big grains, while on metallic surfaces, such as Co and Ru, the Cu atoms adhere strongly to the surface and diffuse slowly.

The effect of precursor exposure time on the film surface roughness was investigated by atomic force microscopy (AFM). When the copper exposure time increased four times from 1 to 4 s, the copper grain sizes grew from 44 to 69 nm. Increasing the exposure time increased the total time available for diffusion to form larger grains
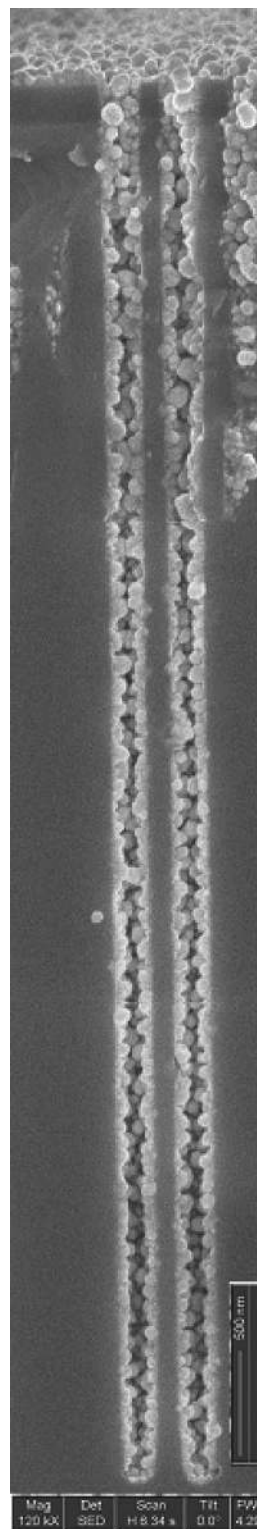

Figure 7. SEM study of ALD Cu over high-aspect-ratio holes (AR ~ 35–40).

with increased roughness. Increasing exposure time did not increase the number of nuclei, because that effect would have resulted in decreasing roughness with increased exposure time. The average thickness, as measured by RBS, did not change when the exposure time was increased, because the surface reactions were already saturated at 1 s.

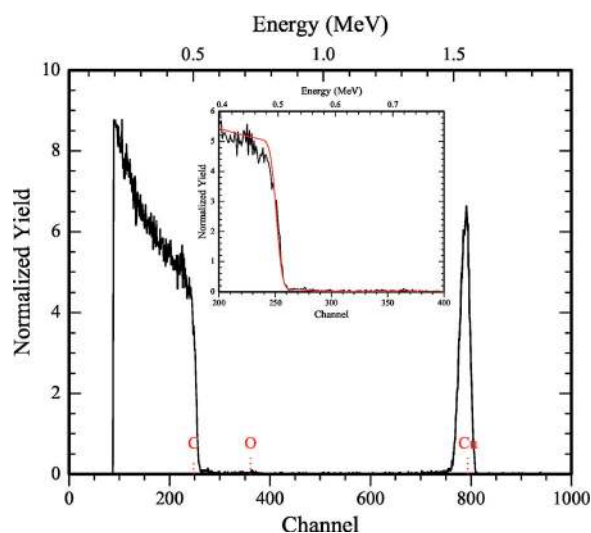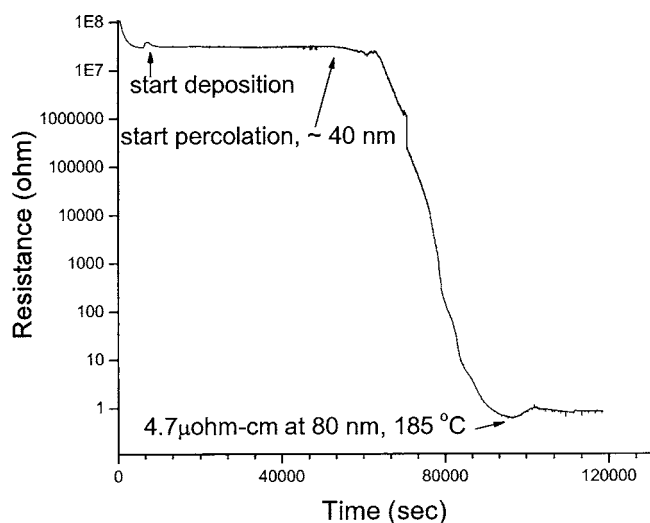The surface roughness of as-deposited film was also temperature-

Figure 8. (Color online) RBS analysis of ALD Cu films on glassy carbon substrates.

Figure 9. High-resolution TEM image of a polycrystalline copper nucleus. Scale bar is 5 nm.

dependent. Figure 11 showed the surface morphologies of copper films deposited on ruthenium surface at different temperatures. The deposition conditions were the same for all of the depositions, except for the deposition temperature. At 150°C, the film has RMS roughness of 1.5 nm at an average thickness of 5.1 nm. When the temperature was increased to 190°C, the film became rougher, having an RMS roughness of 3.0 nm with a thickness of 3.4 nm. When the temperature was further increased to 280°C, the film roughness increased to 21.1 nm at an average thickness of 4.7 nm. Therefore, copper nuclei diffusion was much faster at higher temperatures, leading to bigger grains and rougher surfaces.

Film continuity and electrical conductivity are very important for seed layers in interconnect applications. The copper films were shiny metallic and specular in reflection and electrically conductive. The sheet resistance of the as-grown copper films was investigated by both in situ and ex situ four-point measurements. Scheme 2 showed the in situ four-point measurement of the sheet resistance change during the copper growth on glass surface at 185°C. The sheet resistance decreased eight orders of magnitude from entirely insulating (10^8 $\Omega/\square$) to very conductive copper film at the end

(<5 $\Omega/\square$). The film became conductive at a thickness around 40 nm. This high percolation thickness for copper on glass confirms poor nucleation and agglomeration on the oxide surface. The resistivity of the film reached 4.7 $\mu\Omega$-cm at a thickness of 80 nm, corresponding to a resistivity of 2.9 $\mu\Omega$-cm at room temperature.

ALD copper has denser nucleation and smoother surface morphology on metallic surfaces, leading to lower resistivity. Figure 12 shows the resistivity of copper films on Ru substrates, along with values from very pure copper films sputtered in high vacuum (2 square dots)[19] and the copper film from the reduction of copper nitride (round dots).[20] ALD copper films have slightly higher resistivity ($\sim$20%) compared with PVD copper or copper from the reduction of Cu_3N. The surface of ALD Cu films was rougher than those from sputtering or from copper nitride reduction, which could increase resistance due to surface scattering. The comparable results indicate high-quality copper films were made from the ALD technique, including high purity, continuity of structure, and lack of agglomeration on Ru surfaces.

The resistivity of metal thin films increases with decreasing film thickness due to several scattering effects, such as grain boundary scattering and electron-surface scattering. The curve in Fig. 12 was fitted with a model that includes grain boundary scattering[21]

$$\rho/\rho_0 = 1 + 1.5[R/(1-R)]\lambda/g$$

where ρ_0 is the bulk resistance, λ is the electron mean-free-path ($\sim$40 nm) in bulk copper, g is the average size of the grains, taken here as the film thickness, and $R \sim 0.3$ is the scattering coefficient at grain boundaries.[22] It is remarkable that the ALD copper data is comparable to this model down to a thickness of $\sim$1 nm, or only about four monolayers of copper atoms. This agreement between the measured conductivity and the model suggests that the copper films must be nearly uniformly covering the ruthenium surface even at a thickness of only a few atomic layers of copper.

Scheme 2. In situ resistance measurement of as-deposited Cu film with time and thickness at 185°C on a glass surface.

Growth Mechanism
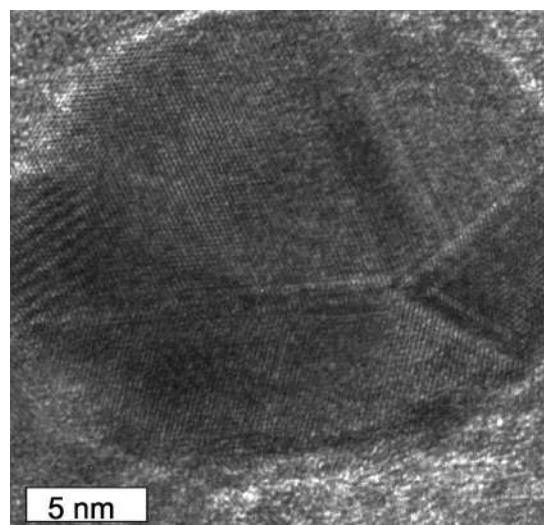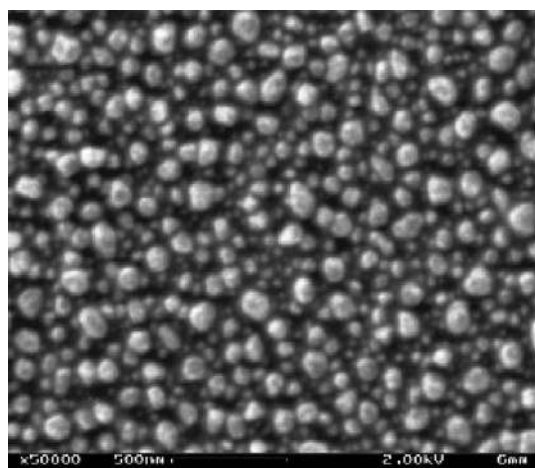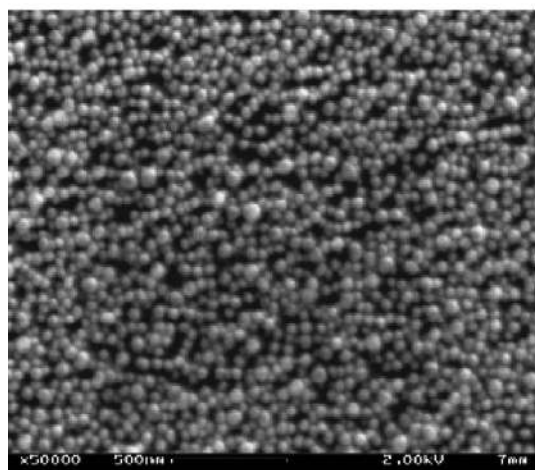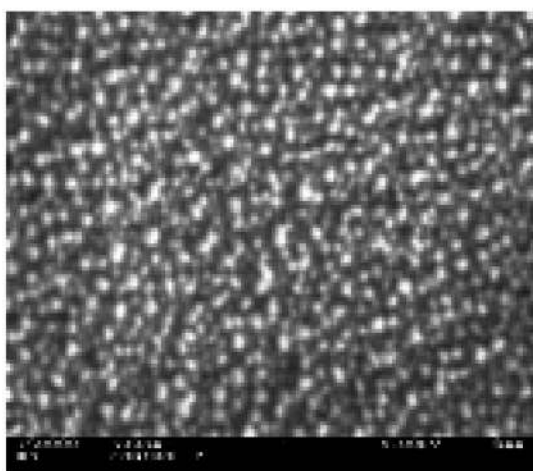
The growth mechanism of ALD metal processes is complex. ALD Cu nucleates poorly on oxide surfaces and agglomerates but the initial growth per cycle is high, approaching a monolayer per cycle. In contrast, the nucleation of copper is dense and smooth on metallic Co and Ru surfaces but the growth per cycle is lower. The rapid growth on oxide surfaces may arise because copper atoms and chemisorbed precursors rapidly diffuse and self-agglomerate to form
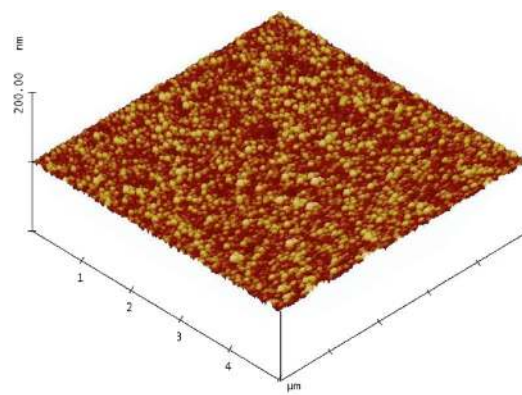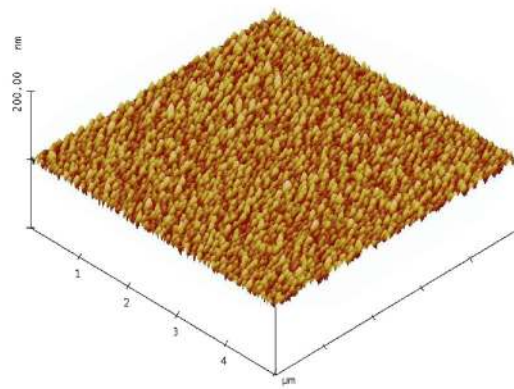
(a)

(b)

(c)

Figure 11. (Color online) AFM study of temperature-dependent surface nucleation of ALD Cu on sputtered Ru substrates: (a) T_{dep} = 150°C, thickness 5.1 nm, RMS roughness 1.5 nm, (b) T_{dep} = 190°C, thickness 3.4 nm, RMS roughness 3.0 nm, and (c) T_{dep} = 280°C, thickness 4.7 nm, RMS roughness 21 nm.

(a)

(b)

(c)

Figure 10. SEM study of surface morphology of ALD Cu on different substrates: (a) on glass, (b) on ALD deposited WN surface, and (c) on ALD-deposited Co.
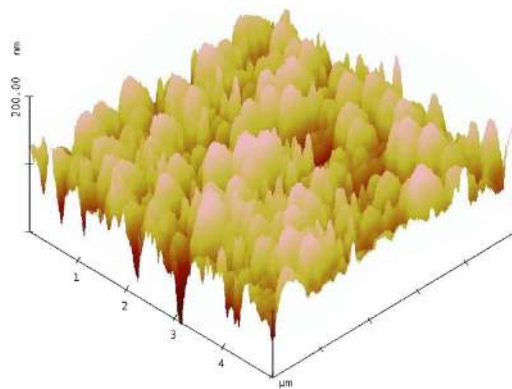
large copper nuclei, opening up access to additional reactive sites (most likely –OH groups) at which more copper precursors react. On metallic surfaces, copper atoms have strong adhesion to the underneath metallic atoms, so they do not diffuse to form large nuclei.

This slows growth on metals, because the chemisorbed precursors block access to neighboring sites and inhibit further reaction.

Experiments also showed almost no growth of ALD Cu on HF-last Si surfaces, which consist mainly of Si–H. As a comparison experiment, a nuclear magnetic resonance (NMR) study showed that in benzene-d_6 solution Cu(I) amidinates reacted with triethylsilanol, Et$_3$SiOH, immediately at room temperature but reacted hardly at all with triethylsilane, Et$_3$SiH. This confirmed that the Cu precursor can readily react with Si–OH groups but not with Si–H groups, which are chemically similar to Si–H terminated silicon surfaces.

In order to study the overall chemistry of the ALD process, hydrogen was periodically introduced to liquid Cu amidinate at 120°C.
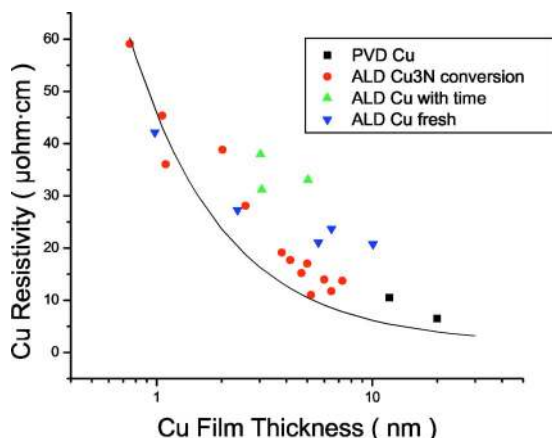
Figure 12. (Color online) ALD Cu film resistivity as a function of film thickness.

After the reaction completed, the products included copper metal (a film on surfaces and a dark powder), along with a liquid by-product. The liquid was confirmed by NMR to be the hydrogenated ligand, N,N'-di-sec-butylacetamidine.

Thus, we find that the overall chemistry goes according to the following equation
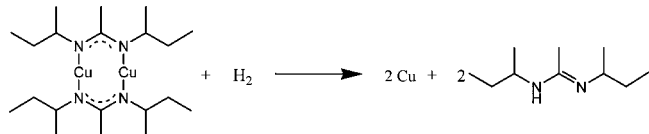
Conclusions

A new group of copper(I) amidinates were characterized and used as precursors for ALD of Cu. Among them, Cu(I) N,N'-di-sec-butylacetamidinate was especially attractive due to its low melting point, high volatility, thermal stability, and high reactivity to surfaces previously treated with molecular hydrogen. Besides the volatility and thermal stability advantages, this Cu(I) amidinate provides additional benefits for ALD Cu applications over traditional metal chlorides and copper β-diketonate derivatives. The precursor is a liquid during evaporation, which gives reproducible vapor pressure, leading to reliable and consistent film depositions. The compound contains highly reactive Cu–N bonds, rather than Cu–C and Cu–O bonds, leading to less carbon and oxygen contamination. It reacts readily with molecular hydrogen, which allowed the ALD copper process at low temperatures (150–190°C). At low temperatures the films are smoother and more conductive. At temperatures below 120°C, there is no copper deposition, so the warm walls of a reactor stay clean of unwanted deposition. The byproduct amidine vapors were not corrosive to the substrates or reactors.

The carbon and oxygen impurities were both low enough to give highly conductive copper films. The resistivity of ALD copper is comparable to very pure PVD copper films and agreed with a grain-boundary scattering model. ALD copper nucleates well on metallic cobalt and ruthenium surfaces, on which the copper is continuous and conductive at thicknesses of <1 nm. With 4 nm copper on top of 2 nm ruthenium, the sheet resistance can be low enough (<50 Ω/□) for use as a seed layer for electroplating copper in metallization for microelectronics.

The conformality of ALD techniques can overcome the limitations of the physical vapor methods to make conformal thin films in narrow trenches required in smaller electronic devices. This process should make it possible to extend the current electroplating process to devices with much smaller features.

References

1. R. Rosenberg, D. C. Edelstein, C. Hu, and K. P. Rodbell, *Annu. Rev. Mater. Sci.*, **30**, 229 (2000).
2. T. Kodas and M. Hampden-Smith, *The Chemistry of Metal CVD*, VCH Publishers, Inc., Weinheim (1994).
3. H. Kim, *Surf. Coat. Technol.*, **200**, 3104 (2006).
4. R. Puurunen, *J. Appl. Phys.*, **97**, 121301 (2005).
5. C. Jezewski, W. A. Lanford, C. J. Wlegand, J. P. Singh, P.-I. Wang, J. J. Senkevich, and T.-M. Lua, *J. Electrochem. Soc.*, **152**, C60 (2005); A. Niskanen, A. Rahtu, T. Sajaavaara, K. Arstila, M. Ritala, and M. Leskela, *J. Electrochem. Soc.*, **152**, G25 (2005).
6. M. Juppo, M. Ritala, and M. Leskela, *J. Vac. Sci. Technol. A*, **A15**, 2330 (1997).
7. P. Martensson and J. O. Carlsson, *Chem. Vap. Deposition*, **3**, 45 (1997).
8. A. U. Mane and S. A. Shivashankar, *Mater. Sci. Semicond. Process.*, **7**, 343 (2004).
9. P. Martensson and J. O. Carlsson, *J. Electrochem. Soc.*, **145**, 2926 (1998).
10. Z. Li, S. T. Barry, and R. G. Gordon, *Inorg. Chem.*, **44**, 1728 (2005).
11. T. Ozawa, *Thermochim. Acta*, **174**, 185 (1991); A. Devi and S. A. Shivashankar, *J. Therm Anal. Calorim.*, **55**, 259 (1999).
12. M. F. Richardson and R. E. Sievers, *Inorg. Chem.*, **10**, 498 (1971).
13. L. A. Torres-Gomez, G. Barreiro-Rodriguez, and A. Galarza-Mondragon, *Thermochim. Acta*, **124**, 229 (1988).
14. R. G. Gordon, D. M. Hausmann, S. Kim, and J. Shepard, *Chem. Vap. Deposition*, **9**, 73 (2003).
15. Z. Li, R. G. Gordon, D. F. Farmer, Y. Lin, and J. Vlassak, *Electrochem. Solid-State Lett.*, **8**, 1 (2005).
16. C. V. Thompson, *Annu. Rev. Mater. Sci.*, **20**, 245 (1990).
17. S. Vaidya and A. K. Sinha, *Thin Solid Films*, **75**, 253 (1981).
18. M. P. Hughey, D. J. Morris, R. F. Cook, S. P. Bozeman, B. L. Kelly, S. L. N. Chakravarty, D. P. Harkens, and L. C. Stearns, *Eng. Fract. Mech.*, **71**, 245 (2004).
19. S. Rossnagel and T. S. Kuan, *J. Vac. Sci. Technol. B*, **22**, 240 (2004).
20. Z. Li and R. G. Gordon, *Chem. Vap. Deposition*, **12**, 435 (2006).
21. T. S. Kuan, C. K. Inoki, G. S. Oehrlein, K. Rose, Y. Zhao, G. Wang, S. M. Rossnagel, and C. Cabral, *Mater. Res. Soc. Symp. Proc.*, **612**, D7.1.1 (2000).
22. J. M. Harper, C. Cabral, P. C. Andricacos, L. Gignac, I. C. Noyan, K. P. Rodbell, and C. K. Hu, *J. Appl. Phys.*, **86**, 2516 (1999).